Chem. Senses 28: 509–522, 2003

Extracellular Transduction Events Under Pulsed Stimulation in Moth Olfactory Sensilla

Jean-Pierre Rospars[1,2], Petr Lánský[3,5] and Vlastimil Křivan[4,5]

[1]Unité de Phytopharmacie et Médiateurs chimiques, INRA, 78026 Versailles Cedex, [2]Unité BIA, INRA, 78352 Jouy-en-Josas Cedex, France, [3]Institute of Physiology, Academy of Sciences, Videnska 1083, 14220 Prague 4, [4]Institute of Entomology, Academy of Sciences and [5]Faculty of Biological Sciences, USB, Branisovská 31, 37005 Ceské Budejovice, Czech Republic

Correspondence to be sent to: J.-P. Rospars, Unité de Phytopharmacie et Médiateurs chimiques, INRA, 78026 Versailles Cedex, France. e-mail: rospars@versailles.inra.fr

Abstract

In natural conditions, pheromones released continuously by female moths are broken in discontinuous clumps and filaments. These discontinuities are perceived by flying male moths as periodic variations in the concentration of the stimulus, which have been shown to be essential for location of females. We study analytically and numerically the evolution in time of the activated pheromone-receptor (signaling) complex in response to periodic pulses of pheromone. The 13-reaction model considered takes into account the transport of pheromone molecules by pheromone binding proteins (PBP), their enzymatic deactivation in the perireceptor space and their interaction with receptors at the dendritic membrane of neurons in *Antheraea polyphemus* sensitive to the main pheromone component. The time-averaged and periodic properties of the temporal evolution of the signaling complex are presented, in both transient and steady states. The same time-averaged response is shown to result from many different pulse trains and to depend hyperbolically on the time-averaged pheromone concentration in air. The dependency of the amplitude of the oscillations of the signaling complex on pulse characteristics, especially frequency, suggests that the model can account for the ability of the studied type of neuron to resolve repetitive pulses up to 2 Hz, as experimentally observed. Modifications of the model for resolving pulses up to 10 Hz, as found in other neuron types sensitive to the minor pheromone components, are discussed.

Key words: intensity coding, neuron modelling, olfaction, pheromone, receptor, temporal coding

Introduction

The present paper is based on two lines of thought. The first one comes from the realization that temporal discrimination is an essential feature of odorant perception in insects. It has been shown in natural conditions that air turbulence physically breaks the initially continuous pheromone plume into spatially and temporally discontinuous patches (Murlis *et al.*, 1992). For an insect flying in the plume the discontinuities appear as a temporally structured signal. Males of *Bombyx mori* orient upwind only when the signal is pulsed (Kramer, 1986, 1992). Behavioral (Kennedy *et al.*, 1980, 1981; Willis and Baker, 1984; Vickers and Baker, 1992) and neurophysiological (Christensen and Hildebrand, 1988; Rumbo and Kaissling, 1989; Marion-Poll and Tobin, 1992; Kodadová, 1996) experiments indicate that the optimum frequency of the periodic stimulation is in the range 1–10 Hz.

The second line of thought comes from the recent progress in the understanding of perireceptor and receptor events [reviewed in (Stengl *et al.*, 1999)]. On this basis, Kaissling (Kaissling, 2001) proposed an integrated model of the network of reactions taking place up to receptor activation, in the case of the receptor neuron of the moth *Antheraea polyphemus* sensitive to the main component of the sexual pheromone. Significant improvements have been brought with respect to previous models (Kaissling, 1998a,b; Rospars *et al.*, 2000; Lánský *et al.*, 2001; Křivan *et al.*, 2002). These improvements are qualitative, with the introduction of pheromone binding protein (PBP) and of a more realistic deactivation of the pheromone molecules which can be removed by two enzymatic reactions, the first one (enzyme E) degrading the free ligand, the other one (hypothetical enzyme N) deactivating the PBP–ligand complex. They are also quantitative with the estimation of all reaction rate constants involved in the system.

Putting the two lines of thought together led us to determine the properties of the activated receptor complex resulting from this realistic network of reactions under periodic pulse stimulation. We investigate how the concentration of the complex evolves in time during the transient and steady

states. The static and oscillating components in both states are distinguished and their temporal and concentration characteristics are determined. We are especially interested in the amplitude of the oscillations of the receptor complex in the cell type sensitive to the main component of the pheromone which follows pulses only up to ~2 Hz (Rumbo and Kaissling, 1989; Kodadová, 1996). We extend this investigation to two other cell types sensitive to the minor components (Meng *et al.*, 1989) which are able to discriminate pulses up to 10 Hz. Clearly, intuitive understanding of the behavior of such systems is difficult and only quantitative simulations can lead to definite conclusions.

Model

Reaction network

Schematically the model involves two types of reactions: the activating reactions and the deactivating ones (Table 1). The activating reactions form the main sequence. This sequence starts with the pheromone molecules (ligand) in the air. The molecules that are adsorbed on the cuticle can diffuse at the surface of the olfactory hairs (Kaissling, 1987), cross the cuticle through small pores (Steinbrecht, 1997) and finally reach the sensillum lymph. In Table 1 this is modelled as translocation from air (L_{air}) to perireceptor space (L). Pheromone molecules then react with the reduced form B_{red} of the pheromone binding protein PBP (Pelosi and Maida, 1995; Ziegelberger, 1995) that protects and transports them to the neuron membrane where the PBP–ligand complex reacts with the receptor protein in a two-step reaction (binding and activation). The deactivating reactions are catalyzed reactions in which the active form L of the ligand is deactivated into inactive forms Ł, LB_{ox} and ŁB_{ox}, where B_{ox} stands for the oxidized form of the PBP molecule (Kaissling, 1998b).

The set of differential equations describing this system is given in Appendix A. The variables of interest are L (free ligand in sensillum lymph), LB_{red} (ligand bound to PBP, denoted P), $LB_{red}R$ (LB_{red} bound to receptor, denoted O) and principally $LB_{red}R^*$, the activated form of the receptor protein. We denote C this activated (signaling) complex and $C(t)$ its concentration at time t. The perireceptor and receptor network so defined is only part of a larger system which is preceded by cuticular adsorption and diffusion, and followed by biochemical transduction (amplifying stage) and electric phenomena (conduction of the signal along the dendrite and soma of the receptor neuron). The latter steps are not taken into account here.

The model given in Table 1 was studied in its complete form. However, simulations showed that, at least with used parameter values, some reactions have only a very small influence on concentration $C(t)$. These are called 'secondary reactions' in Table 1.

Table 1 Kaissling's (2001) redox model for reactions involved in perireception and reception of pheromone molecules in the moth *Antheraea polyphemus*[a]

Main reactions	
Activation[b]:	$L_{air} \overset{k_1}{\rightsquigarrow} \overset{B_{red}}{\underset{}{+}} L \underset{k_{-2}}{\overset{k_2}{\rightleftarrows}} LB_{red} \overset{R}{\underset{}{+}} \underset{k_{-3}}{\overset{k_3}{\rightleftarrows}} LB_{red}R \underset{k_{-4}}{\overset{k_4}{\rightleftarrows}} LB_{red}R^*$
Deactivation[c]:	$\overset{N}{\underset{}{+}} LB_{red} \underset{k_{-5}}{\overset{k_5}{\rightleftarrows}} LB_{red}N \overset{k_6}{\rightarrow} \overset{E}{\underset{N}{+}} LB_{ox} \underset{k_{-10}}{\overset{k_{10}}{\rightleftarrows}} LB_{ox}E \overset{k_{11}}{\rightarrow} LB_{ox} \overset{}{\underset{E}{+}}$
Deactivation[d]:	$\overset{E}{\underset{}{+}} L \underset{k_{-8}}{\overset{k_8}{\rightleftarrows}} LE \overset{k_9}{\rightarrow} \text{Ł} \overset{}{\underset{E}{+}}$
Secondary reactions	
Deactivation[e]:	$\overset{E}{\underset{}{+}} LB_{red} \underset{k_{-12}}{\overset{k_{12}}{\rightleftarrows}} LB_{red}E \overset{k_{13}}{\rightarrow} \text{Ł}B_{red} \overset{}{\underset{E}{+}}$
Feedback	$\overset{B_{ox}}{\underset{}{+}} L \underset{k_{-7}}{\overset{k_7}{\rightleftarrows}} LB_{ox}$

[a]With the notation used the main reactant (pheromone L) and its products are written on the line. The other reactants appear above the line and the other products below the line.

[b]First sequence: activating reactions. Pheromone molecules (L) in the sensillum lymph bind to the reduced form (B_{red}) of the pheromone binding protein (PBP). The complex LB_{red} binds to the receptor molecule R and activates it ($LB_{red}R^*$). Initial translocation reactions $L_{air} \rightsquigarrow L_{cut} \rightsquigarrow L_{pore} \rightsquigarrow L$, i.e. adsorption of pheromone molecules in air (L_{air}) on the cuticle (L_{cut}) and diffusion through pores to the sensillum lymph (L), are not detailed here.

[c]Second sequence: deactivation reactions of L bound to PBP. The complex LB_{red} binds to the hypothetical enzyme N which catalyzes its conversion into the oxidized form LB_{ox}. This complex is then degraded by enzyme E into ŁB_{ox}.

[d]Degradation by enzyme E of free L in Ł. The reaction network is incomplete for Ł, which accumulates.

[e]Degradation by enzyme E of LB_{red} in ŁB_{red}. The network is also incomplete for PBP because B_{ox} and B_{red} are not regenerated from the end products LB_{ox}, ŁB_{ox} and ŁB_{red} which consequently also accumulate.

Parameter values

Kaissling was able to determine the values of all the parameters in the model (Table 2) for the cell type sensitive to the main pheromone component (*E*,*Z*-6,11-hexadecadienyl acetate) of the saturniid moth *Antheraea polyphemus* (Kaissling, 2001). These values come from three sources: (i) biochemical experiments, as reported in the literature or done by the author and his co-workers; (ii) electrophysiological experiments, based mostly on measurements of the receptor potential and the elementary receptor potentials (transient potential changes which are thought to result from single receptor protein activations); and (iii) calculations based on the steady-state solution of the model and several approximations. Obtaining such values is a difficult task because it is based on a deep familiarity with

Table 2 Values of parameters used in numerical simulations of the cell type sensitive to main pheromone component (*E*,*Z*-6,11-hexadecadienyl acetate) of *Antheraea polyphemus*, from Kaissling (Kaissling, 2001)

Protein concentrations[a]	
$R_0 = 1.64\ \mu M$	
$B_{red} = 3500\ \mu M$	$B_{ox} = 500\ \mu M$
$N = 1\ \mu M$	$E = 0.4\ \mu M$
Rate constants[b]	
$k_i = 2.9 \times 10^4\ s^{-1}$[c]	
$k_2 = 0.17\ s^{-1}\ \mu M^{-1}$	$k_{-2} = 0.01\ s^{-1}$
$k_3 = 0.209\ s^{-1}\ \mu M^{-1}$	$k_{-3} = 7.9\ s^{-1}$
$k_4 = 16.8\ s^{-1}$	$k_{-4} = 98\ s^{-1}$
$k_5 = 4\ s^{-1}\ \mu M^{-1}$	$k_{-5} = 98.9\ s^{-1}$
$k_6 = 29.7\ s^{-1}$	
$k_7 = 1.7 \times 10^{-4}\ s^{-1}\ \mu M^{-1}$	$k_{-7} = 10^{-5}\ s^{-1}$
$k_8 = 150\ s^{-1}\ \mu M^{-1}$	$k_{-8} = 300\ s^{-1}$
$k_9 = 30\ s^{-1}$	
$k_{10} = 0.15\ s^{-1}\ \mu M^{-1}$	$k_{-10} = 300\ s^{-1}$
$k_{11} = 30\ s^{-1}$	
$k_{12} = 0.15\ s^{-1}\ \mu M^{-1}$	$k_{-12} = 300\ s^{-1}$
$k_{13} = 30\ s^{-1}$	

[a]The concentration of the membrane receptors R_0 is expressed with respect to the volume of the hair $V = 2.6 \times 10^{-12}$ l (Keil, 1984).

[b]See corresponding reactions in Table 1. Forward reactions (left, with positive subscript) and backward reactions (right, with negative subscript).

[c]Translocation rate constant (Kaissling, personal communication).

the system. For this reason and for the sake of comparison, we have taken the parameter values as originally published. However, to account for the temporal characteristics of cell types responding to the minor pheromone components (*E*,*Z*-6,11-hexadecadienal and *E*,*Z*-4,9-tetradecadienal), we studied also a modified set of parameter values.

Constant stimulation

Although the subject of this paper is pulsed stimulation, the response to a periodic stimulus cannot be understood without reference to the simpler constant (or step) stimulation. When the system is stimulated at constant ligand concencentration from time zero, the concentration $C_c(t)$ of the signaling complex initially increases, then approaches a constant level. As shown in Appendix B, this equilibrium response, denoted $\overline{C}_c$, was determined without approximations as a result of a long but straightforward calculation and found to be a hyperbolic function (equation B3 or B6) of the constant concentration of ligand L_c in air surrounding the antenna. This steady-state concentration of the signaling complex $\overline{C}_c$ is not a quantity of much behavioral interest, but is an important reference value from a theoretical point of view. These symbols and all those introduced below are defined in Table 3.

Pulsed stimulation

The concentration of ligand in the air surrounding the antenna is described by periodically repeated square pulses, in the form

$$L_{air}(t) = \begin{cases} L_H & \text{for } t \in \left[j(t_L + t_H), j(t_L + t_H) + t_H \right] \\ 0 & \text{elsewhere} \end{cases} \quad (1)$$

where $j = \{0, 1, \ldots\}$, t_H is the duration of the pulses (at concentration L_H), t_L is the inter-pulse duration. It follows from (1) that any stimulation protocol is characterized by the triplet (L_H, t_H, t_L). The stimulation frequency is

$$f = (t_L + t_H)^{-1} \quad (2)$$

Thus, the stimulation frequency (2) can be changed either by modifying t_L or t_H. The temporal average of the concentration of ligand in air is

$$\overline{L} = L_H \frac{t_H}{t_H + t_L} \quad (3)$$

When the interpulse t_L decreases and tends to zero, $\overline{L}$ increases and tends to the limiting value L_H, which corresponds to a permanent stimulation.

Concentration of ligand in air and flux from air to perireceptor space

Pheromone molecules in the air can cross the hair wall through pores and reach the perireceptor space in the vicinity of the cell membrane. The rate at which they enter the sensillum lymph can be considered, at any time t, as proportional to the pheromone concentration in air $L_{air}(t)$ expressed in nM:

$$\phi(t) = k_i L_{air}(t) \quad (4)$$

where $\phi(t)$ expressed in μM/s denotes the inward flux of molecules at time t and k_i expressed in s^{-1} is the rate constant characterizing the translocation (Rospars *et al.*, 2000). It follows from (4) that the intensity of stimulation can be equivalently expressed as a concentration in air L_{air} (molarity) or as a flux ϕ (molarity per time unit). For example, a constant stimulation L_c generates a flux $\phi_c = k_i L_c$ and during a pulse of height L_H the flux is $\phi_H = k_i L_H$. Experiments in *Antheraea* with ^{3}H-labeled pheromone lead to $k_i = 2.9 \times 10^4\ s^{-1}$ (K.-E. Kaissling, personal communication). Note that this value is smaller than the value $k_i = 10^6\ s^{-1}$ used in our previous work (Rospars *et al.*, 2000). We will use Kaissling's estimate in the present work. With this rate a concentration of 1 nM corresponds to a flux of 29 μM/s. In the following, concentration L_{air} is always expressed in nM and flux ϕ in μM/s.

Table 3 List of main symbols and abbreviations

Symbol	Definition	Unit
A	amplitude of oscillations of C for periodic pulse stimulation	μM
B_{ox}, B_{red}	pheromone binding protein (PBP), oxidized and reduced forms	–
B_{ox}, B_{red}	concentrations of B_{ox} and B_{red}	μM
C	activated receptor complex $LB_{red}R^*$	–
$C(t)$	concentration of C at time t in response to pulsed stimulation	μM
$\overline{C}$	time-averaged concentration of $C(t)$ over one period at steady state	μM
$C_c(t)$	concentration of C at time t in response to step stimulation L_c	μM
$\overline{C}_c$	equilibrium concentration of $C_c(t)$	μM
C_{max}	maximum of $\overline{C}_c$ and $\overline{C}$, asymptote of $\overline{C}_c$ vs. L_c and $\overline{C}$ vs. $\overline{L}$ curves	μM
CD	concentration detector	–
E	enzyme deactivating L (in L) and LB_{ox} (in LB_{ox})	–
FD	flux detector	–
GFD	generalized flux detector	–
f	frequency of stimulation, $f = 1/T$	Hz
k_j	rate constants of the 13 reactions (21 constants, see Tables 1 and 2)	s^{-1}, s^{-1} μM^{-1}
K_D	apparent equilibrium dissociation constant for $\overline{C}_c$ vs. L_c, $K_D \equiv L_{50}$	μM
K_j	equilibrium dissociation constant of reaction j, $K_j = k_{-j}/k_j$	μM
L	ligand *E*,*Z*-6,11-hexadecadienyl acetate (main pheromone component)	–
Ł	metabolic products resulting from enzymatic degradation of L	–
$L(t)$	concentration of L in perireceptor space (lymph) at time t	μM
$L_{air}(t)$	concentration of L in air at time t	nM
$\overline{L}$	time-averaged concentration of L in air over one period (pulsed stim.)	nM
L_c	constant concentration of L in air (step stimulation)	nM
L_H	constant concentration of L in air during pulses (pulse height)	nM
N	hypothetical enzyme deactivating LB_{red} into LB_{ox}	–
$\phi(t)$	flux of L from air into perireceptor space at time t, $\phi(t) = k_i L_{air}(t)$	μM/s
ϕ_c	time-averaged constant flux of L into perireceptor space, $\phi_c = k_i L_c$	μM/s
ϕ_H	constant flux of L into perireceptor space during pulses, $\phi_H = k_i L_H$	μM/s
ϕ_{50}	apparent equilibrium dissociation constant for C_{eq} vs. ϕ_c, $\phi_{50} = k_i K_D$	μM/s
R	receptor of L on the neuron membrane	–
R_0	concentration of R with respect to the sensillum volume	μM
t_H	pulse duration	ms
t_L	interpulse duration	s or ms
T	period of stimulation, $T = t_H + t_L$	s or ms

Results

All numerical results are based on the constants given in Table 2, except those in the section on 'Modified parameters for a higher temporal resolution'.

Response as a function of time

When periodic pulses of ligand molecules in air are applied to the system, the concentration $L(t)$ of free ligand in the perireceptor space follows the stimulus without much distortion (Figure 1A). This is not the case of the concentrations of the three next species along the activation pathway, $P(LB_{red})$, $O(LB_{red}R)$ and $C(LB_{red}R^*)$, which all initially increase for several periods, then reach steady-state oscillations (Figure 1). Now, these 'steady' states are actually periodic, $P(t)$, $O(t)$ and $C(t)$ fluctuating around constant values with different amplitudes and the same period T. Period T is always equal to that, $t_L + t_H$, of the stimulation (Figure 2). This means that the intermediate species and the signaling complex merely follow, with a time lag and a more or less severe deformation, the time course of the stimulus. The responses oscillate between a lower bound (trough) and an upper bound (crest). During each pulse the response increases and tends to a horizontal asymptote that can be closely approached only if the pulse is of sufficiently long duration. Then, the response decays and tends to the zero level, which similarly can be reached only if the interpulse is sufficiently long. For all stimulations shown in Figure 2, the response of the complete system, with all 13 reactions, is practically identical to the response of the simplified 10-reaction system shown in Table 1 (main reactions).

Because the concentrations fluctuate around average levels they can be analyzed as the sum of a monotonic component (average of response over one period), which is studied in the next two sections, and an oscillating component, examined in the two final sections. For the sake of

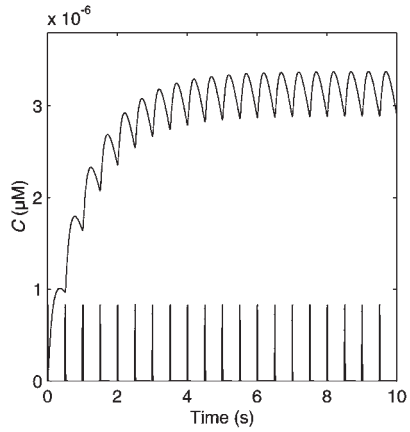

Figure 1 Concentrations of activated receptors $C(t)$ as a function of time. Amplitude of C at steady state is 2.43×10^{-7} μM (0.38 molecules/cell). Bottom trace shows the timing of the odor pulses (height of pulses is not to scale). *Input variables:* $L_H = 3.4 \times 10^{-4}$ nM in air (i.e. flux 10^{-2} μM/s), t_H = 20 ms, t_L = 480 ms; thus $L_c = 1.36 \times 10^{-5}$} nM and f = 2 Hz, maximum frequency of cell type sensitive to main pheromone component. *Parameters:* as in Table 2. In this and other figures, the flux from air into perireceptor space expressed in μM/s is 29 times the concentration in air expressed in nM.

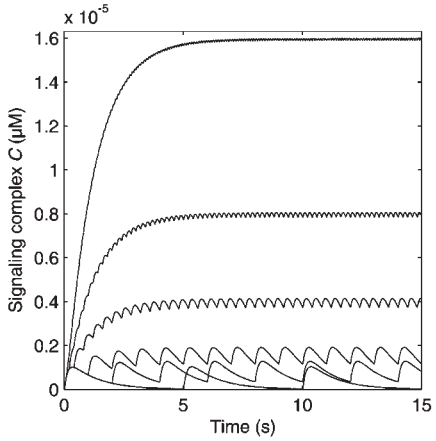

Figure 2 Concentrations of the signaling complex, $C(t)$, as a function of time for different frequencies of stimulation f. The transient and steady states are shown for the same pulse height L_H and duration t_H at different interpulse t_L. $C(t)$'s oscillate between an upper bound and a lower bound. Except for t_L = 4.98 s decay to level close to zero is not observed because the pulse trains are too fast to allow the response to develop with full amplitude. *Input variables:* $L_H = 3.4 \times 10^{-4}$ nM (i.e. $\phi_H = 10^{-2}$ μM/s), t_H = 20 ms, and from bottom to top t_L = {4.98, 1.98, 0.98, 0.38, 0.18, 0.08 s} or equivalently f = {0.2, 0.5, 1, 2.5, 5, 10 Hz} . Note that 20 ms pulses merge in a continuous stimulation at 50 Hz. For t_H and t_L fixed, the relative positions of the curves and their relative amplitudes remain identical to those shown here in the range $0 < \phi_H < 100$ μM/s. *Parameters:* as in Table 2.

simplicity only the concentration $C(t)$ of the signaling complex $LB_{red}R^*$ is studied in detail. It is called here the response of the system.

Monotonic component of the response during the steady state

Once the steady state is reached, the (constant) monotonic component can be estimated by averaging $C(t)$, over one period T. It can be shown numerically that this average $\overline{C}$ is equal to the equilibrium response $\overline{C}_c$ of the system to a constant stimulation L_c delivering each period the same amount of ligand $\overline{L}$ as the periodic pulses (Figure 3), i.e. $L_c = \overline{L}$, where $\overline{L}$ is given by equation (3). This is a noteworthy simplification for the analysis of the system because it implies that, for studying the monotonic component at steady state, attention can be restricted to constant stimulations without any loss of information. The response $\overline{C}_c$ can be determined exactly (see Appendix B); this is the only feature of the response to a periodic pulsed stimulation that can be derived analytically. It follows from equation (3) that the same mean steady-state level of the signaling complex can be achieved in several ways with pulses of different heights, durations or interpulse lengths.

When $\overline{L}$ increases, $\overline{C}$ also increases as shown in Figure 4. In the standard plot $\overline{C}$ vs. $\overline{L}$, identical to $\overline{C}_c$ vs. L_c (Figure 4A), is a branch of hyperbola that tends to an asymptotic maximum C_{max} given by equation (B4). The ligand concentration at half-maximum response, C/C_{max}=0.5, given by equation (B5), is $K_D = L_{50} \simeq 1$ nM (corresponding to a flux ϕ_{50} = 30.2 μM/s) for parameters of Table 1. In the semilog plot $\overline{C}$ vs. log $\overline{L}$, identical to $\overline{C}_c$ vs. log L_c (Figure 4B), is a logistic curve with an inflection point at K_D. The dynamic range of the curve between L_1 at 1% saturation ($\overline{C}/C_{max}$ = 0.01) and L_{99} at 99% saturation is 4 log units, which is a general property of logistic curves (Rospars *et al.*, 1996). For $\overline{L} \lesssim L_{10}$, i.e. 0.12 nM, the hyperbola can be very well approximated by the straight line given by equation (B7). In this range, the system is practically linear.

Monotonic component of the response during the transient state

The transient response to a periodic stimulus, like the steady state, can be described as the summation of a monotonic component (that yielded by the corresponding step stimulation) and an oscillating one (Figure 5). Thus the characteristics of the monotonic component are those derived from a step stimulation of intensity $L_c = \overline{L}$. How the transient state changes into the steady state $\overline{C}$ for different values of $\overline{L}$, or equivalently $\overline{C}_c$ for different values of L_c, is shown in Figure 5A. It is difficult to judge from this figure whether the time needed to come close to the steady state is the same or not. This can be better seen using the ratio $C(t)/\overline{C}$, which allows one to compare the kinetics of the signaling complex at different stimulation strengths independently of the asymptotic concentrations (Figure 5B). Then it appears that the time to reach the steady state $\overline{C}$ of the signaling complex decreases when $\overline{L}$ increases. For all ligand concentrations $\overline{L} < L_1$ the $C(t)/\overline{C}$ curves are very similar, which means that the duration of their transient

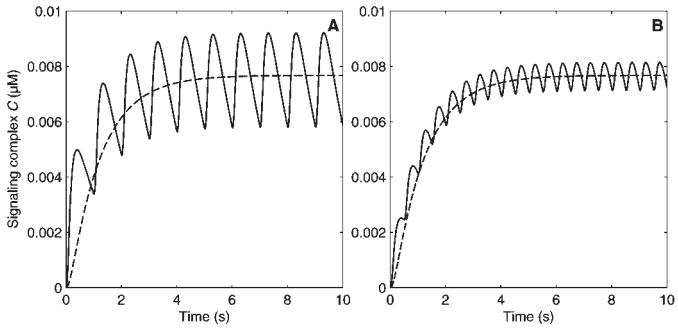

Figure 3 Comparison of the concentrations of the signaling complex in response to a step stimulation $C_c(t)$ (dashed line) and a periodic pulsed stimulation $C(t)$ (solid line) for the same amounts of ligand molecules delivered per time unit at two frequencies 1 Hz **(A)** and 2 Hz **(B)**. For any amount L_c, the height of the periodic pulses is given by $L_H = L_c(t_H + t_L)/t_H$, see equation (3). The response to a step stimulation is always within the range of variation of the response to periodic pulses. The asymptotic level $\overline{C}_c$ for the step stimulation is given by equation (B3); it is equal to that of the periodic response averaged over one period $\overline{C}$. *Input variables:* $L_c = 3.4 \times 10^{-2}$ nM (i.e. $\phi_c = 1$ μM/s), $t_H = 0.1$ s and $t_L = 0.9$ s (1 Hz, A), $t_L = 0.4$ s (2 Hz, B). *Parameters:* as in Table 2.

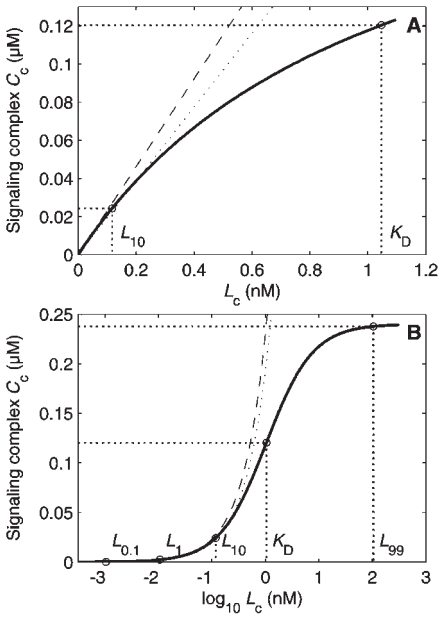

Figure 4 Monotonic component. Mean concentration of the signaling complex in the steady state $\overline{C}_{eq}$ (μM, dashed line in Figure 3) as a function of the concentration of ligand molecules L_c (nM) or corresponding flux ϕ_c (μM/s). L_c can be obtained by various combinations of L_H, t_H and t_L as shown by equation (3). The same curves would be obtained with step stimulations of intensities L_c. **(A)** Hyperbolic curve C_c vs. L_c as given by equation (B3) in Appendix B. Concentrations $L_{10} = 0.117$ nM and $L_{50} = K_D = 1.04$ nM at 10% and 50% respectively of maximum response C_{max} are shown. For $L_c < L_{10}$ the hyperbola is very well approximated by line $C_1 = 0.23L$ (dashed line); line $C_2 = 0.19L$ (dotted line) is slightly better for $L_c > L_{10}$. **(B)** Corresponding logistic curve C_c vs. $\log L_c$, with concentrations $\log L_{0.1} = -3$ ($\log \phi_{0.1} = 1.52$), $\log L_1 = -2$ ($\log \phi_1 = -0.52$), $\log K_D = 0$ ($\log \phi_{50} = 1.48$), $\log L_{99} = 2$ ($\log \phi_{99} = 3.46$) at which 0.1%, 1%, 50% and 99% respectively of $C_{max} = \max(C_c) = 0.24$ μM are reached. Curves C_1 (dashed) and C_2 (dotted) are also shown.

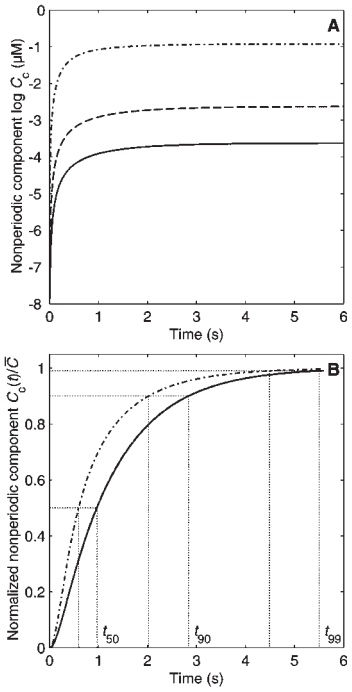

Figure 5 Kinetics of the monotonic component C_c of the signaling complex. **(A)** Concentration C_c as a function of time for various stimulus intensities $L_c = \{L_{0.1}, L_1, L_{50} = K_D\}$ (from bottom to top) (see Figure 4). **(B)** Same curves for relative concentration $C_c(t)/\overline{C}_{eq}$; the curves for $L_{0.1}$ and L_1 (solid line) are superimposed. The times needed to reach half-saturation ($C_{max}/2$), $t_{50} = \{0.6, 0.98$ s$\}$, 90% of saturation, $t_{90} = \{2.05, 2.88$ s$\}$, and 99% of saturation $t_{99} = \{4.55, 5.58$ s$\}$, are indicated. Note that, as shown in Figure 3, the steady-state concentration for a step stimulation is equal to $\overline{C}_c$, the time averaged concentration for periodic pulses, $\overline{C}$, so these graphs are valid for both types of stimulations.

states are very close, ~5.58 s to reach 99% of $\overline{C}$. For K_D the transient time is noticeably shorter, 4.55 s to reach the same 99% level.

Oscillating component of the response during the steady state

The oscillating component of the steady state can be shown in isolation by substracting the response $C_c(t)$ to a step stimulation from the response $C(t)$ to a pulsed stimulation. The oscillating component calculated in this way is shown in Figure 6. The main characteristic of interest, the amplitude of the oscillations, i.e. half of the distance between extrema of $C(t)$, has to be calculated numerically.

Contrary to the average magnitude $\overline{C}$, the amplitude A of the response during the steady state does not depend on the quantity $\overline{L}$ but on the individual characteristics L_H, t_H and t_L of the pulses. Before studying these dependencies it is useful to introduce the notion of the 'natural pulse' of the system; it reverses the usual point of view of observing the response yielded by a specified stimulation by modifying the stimulation in order to obtain a specified response. The periodic stimulus is 'natural' for the system if the pulse duration is

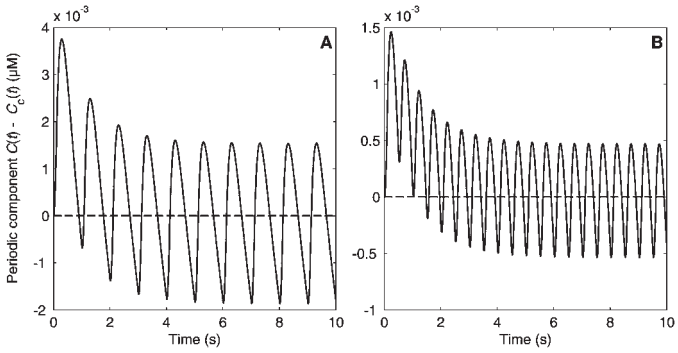

Figure 6 Oscillating component. Oscillation of the signaling complex at the transient and steady states shown in isolation as the difference $C(t) - C_c(t)$, where $C_c(t)$ is the response to the step stimulation corresponding (with same L_c) to the pulsed one giving $C(t)$ (see justification in Figure 3). Two different periodic pulsed stimulations are shown for L_H = 0.34 nM (10 μM/s), t_H = 0.1 s, t_L = 0.9 s in **(A)**, and L_H = 0.17 nM (5 μM/s), t_H = 0.1 s, t_L = 0.4 s in **(B)**; in both cases $L_c = 3.4 \times 10^{-2}$ nM (1 μM/s). The first five or ten oscillations correspond to the transient state and the following ones to the steady state. The duration of the transient state depends only on L_c (see Figure 5). Input variables: same as Figure 3.

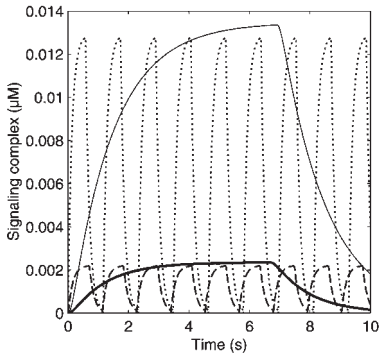

Figure 7 Natural periods of various system components: single-step receptor–ligand interaction ($R + LB_{red} \rightleftharpoons LB_{red}R$ only, one-step CD; dotted line), double-step receptor–ligand interaction ($R + LB_{red} \rightleftharpoons LB_{red}R \rightleftharpoons LB_{red}R^*$, double- step CD; dashed line), and complete system as shown in Table 1, either with standard parameter values (thick solid line), or with k_3 increased 6-fold (thin solid line). Each system was stimulated with a train of square pulses of the same height 10^{-2} nM (0.30 μM/s) and different temporal characteristics. Pulse durations were determined so that at the end of the pulse the concentration of signaling complex ($LB_{red}R$ or $LB_{red}R^*$) was 99% of its equilibrium value $\overline{C}_c$, and the interpulse durations so that this concentration was allowed to decay to 1% of $\overline{C}_c$. These 'natural' periods are 1.16, 1.13, 12.22 and 13.83 s respectively, i.e. natural frequencies are 0.86, 0.88, 0.082 and 0.072 Hz. Periods and relative concentrations would be the same with any pulse height in the linear range, i.e. $\overline{L} < 0.12$ nM (see Fig. 4). *Parameters:* Same as in Table 2, except k_3 which was increased 6-fold (from standard 0.209 to 1.254) for thin solid curve only.

such that $C(t)$, can rise to 99% of its maximum asymptotic value $\widetilde{C}_c$, and the interpulse long enough for $C(t)$ to decay to 1% of $\widetilde{C}_c$. These pulse characteristics define the 'natural frequency' of the system because it is the highest frequency which gives the (almost) maximum possible amplitude. For any higher frequency, the response cannot go so close to the asymptotes and thus the amplitude of the oscillations is only a fraction of the distance between the asymptotes. The natural frequency depends on L_H but in the range of stimulus concentration $\overline{L}$ up to ~0.1 nM in air (i.e. a flux of 3 μM/s), in which the system is practically linear, it is constant, f = 0.082 Hz and the corresponding 'natural period' is T = 12 s (Figure 7). The natural frequency of the whole system is ~10 times lower than that of the receptor–ligand interaction reactions considered in isolation (0.88 Hz), which indicates that the transport and degradation reactions are responsible for this slowing down.

In the simplest case, where both t_H and t_L are longer than in the 'natural pulse', $C(t)$ can first approach the asymptote $\overline{C} = \overline{C}_c$ corresponding to a constant stimulation of intensity $\overline{L}$ (upper bound), then approach zero (lower bound), so that the amplitude is (almost) fully expressed and $A \simeq \overline{C}/2$. Then equation (B3) applies: amplitude A grows hyperbolically with $\overline{L}$ and tends to $C_{max}/2$ when the concentration of activated receptors approaches its maximum. However, for any frequency higher than the natural frequency, the amplitude of the oscillations is limited to a fraction of this range because the pulses stop before the upper bound is reached and start again before decay to the lower bound.

The basic protocol for studying how the amplitude depends on the input variables consists in maintaining the third variable constant (e.g. t_H) and plotting A vs. the first variable (e.g. L_H) for a series of fixed values of the second variable (t_L), in practice different frequencies. Using this approach we investigated how amplitude changes when pulse height L_H is increased for extreme values of t_H (1 and 50 ms; Figure 8) and frequency (1 and 10 Hz; Figure 9).

Figure 8 shows that, for a biologically meaningful range of values of t_H and t_L, $\log A$ first increases linearly with $\log L_H$, reaches a maximum, then decreases linearly (Figure 8A). Equivalently, the relative amplitude $A/\overline{C}$ remains constant then decreases linearly (Figure 8B). The latter representation confirms that, in the left part of the curve, A depends linearly on L_H and that the slope of this straight line is not a constant but depends on f and t_H. The ligand concentration in air at which the maximum amplitude occurs depends on t_H, it is ~3.4 nM (i.e. flux 100 μM/s) for t_H = 100 ms and $\sim 3.4 \times 10^3$ nM (i.e. flux 10^5 μM/s) for t_H = 1 ms.

Figure 8 shows that the amplitude of oscillations depends first of all on pulse height, secondarily on frequency and marginally on pulse duration; the effect of L_H is greater by several orders of magnitude than that of t_H. Practically, only L_H is important since the curves of A for extreme values of t_H and f are very similar (Figure 8A). On the contrary, for relative amplitude $A/\overline{C}$ only frequency is decisive, L_H and t_H being negligible (Figure 8B). The final decline of A for high L_H results from the fact that the 'saturation' of the receptors prevents the upper bound from moving further up while the lower bound of the oscillations still moves up with L_H. It follows from these simulations that the optimum L_H of the

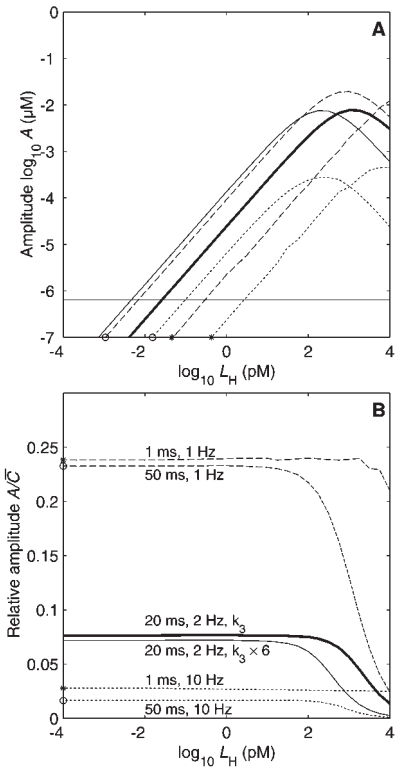

Figure 8 Amplitude of the periodic oscillations of signaling-complex concentration as a function of pulse height L_H. **(A)** Amplitude A vs. height L_H with both axes in log scale, at pulse frequency $f = 2$ Hz, pulse duration $t_H = 20$ ms and either standard k_3 (thick solid line) or k_3 increased 6-fold (thin solid line). Other lines are for comparison at two pulse frequencies, $f =$ 1 Hz (dashed lines) and 10 Hz (dotted lines) and two pulse durations, $t_H =$ 1 ms (stars on horizontal axis) and 50 ms (circles). The horizontal line at $A = 10^{-6.2}$ μM corresponds to activation of a single receptor molecule. Along this line from left to right: (20 ms, 2 Hz, increased k_3), (50 ms, 1 Hz), (20 ms, 2 Hz), (50 ms, 10 Hz), (1 ms, 1 Hz), (1 ms, 10 Hz). **(B)** Same plot for relative amplitude $A/\overline{C}$, with $\overline{C}$ time-averaged steady state concentration of signaling complex. Values for 10 Hz (dotted lines at the bottom) were multiplied by 10. *Parameters:* Same as in Table 2 except k_3 which was increased 6-fold (from standard 0.209 to 1.254) for thin solid curves.

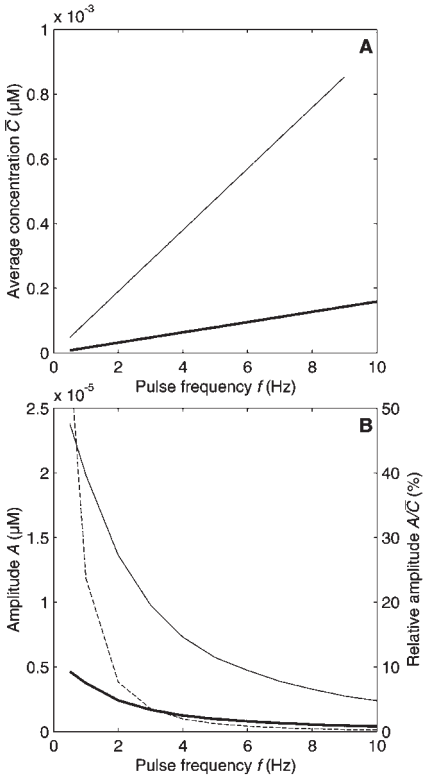

Figure 9 Time-averaged level and amplitude of the oscillating concentration of signaling complex $LB_{red}R^*$ as a function of pulse frequency f between 0.5 and 10 Hz. **(A)** Time-averaged steady-state concentration $\overline{C}$ vs. f for $t_H = 20$ ms and $L_H = 3.4 \times 10^{-3}$ nM (equivalent to $\phi_H = 0.1$ μM/s) for standard k_3 (thick solid line) or k_3 increased 6-fold (thin solid line). $\overline{C} = 10^{-3}$ μM corresponds to 1566 molecules/cell. **(B)** Amplitude A (in μM, solid lines; A $= 2.5 \times 10^{-5}$ μM corresponds to about 40 molecules/cell) and relative amplitude $A/\overline{C}$ (dashed line) as a function of f. Increasing k_3 modifies $\overline{C}$ and A but not $A/\overline{C}$. *Parameters:* Same as in Table 2 except k_3 which was increased 6-fold (from standard 0.209 to 1.254) for thin solid curves only.

system, that which gives the greatest amplitude, is close to L_{99} for $t_H \approx 10$ ms and moves towards K_D for $t_H > 100$ ms.

The amplitude decreases steeply with respect to stimulation frequency (Figure 9B, thick line). This behavior follows from the observation above that, when frequency increases, the signaling complex has not enough time first to reach the upper bound then to return to the lower bound. At the highest frequency resolved by the cell type modeled (2 Hz) (Rumbo and Kaissling, 1989), with 20 ms pulses, the amplitude is 2.42×10^{-6} μM for $L_H = 3.4 \times 10^{-3}$ nM, i.e. flux 0.1 μM/s. It means that the signaling complex fluctuates by 3.8 molecules/cell around its average level which is 50 molecules/cell. These numbers can be considered as compatible with periodic threshold crossing and firing of the cell. However, because the average level of signaling complex $\overline{C}$ grows linearly with frequency (Figure 9A), the relative amplitude declines still faster than amplitude with pulse frequency (Figure 9B, dashed line), so that the oscillations become progressively lost on top of a growing steady-state number of activated molecules. For example, amplitude is reduced four times (0.95 activated molecules/cell for an average of 12 activated molecules/cell) with a 4-fold decrease of pulse height and about 4 times (0.86 molecules/cell for an average of 200) with a 4-fold increase of frequency. So, the cell becomes unable to follow pulses either because the amplitude falls below one activated receptor molecule per cell, at low ligand concentration, or because the relative amplitude becomes too small, at high concentration.

Oscillating component of the response during the transient state

The oscillating component of the transient state can be shown in isolation by substracting the response $C_c(t)$ to a step stimulation from the transient response $C(t)$ under pulsed stimulation. As seen before, response $C_c(t)$ grows to constant $\overline{C}_c$, whereas $C(t)$ finally oscillates around the same

Table 4 Concentration $\overline{C}$ and amplitude A of signaling complex $LB_{red}R^*$ at steady state[a]

k_3 (s^{-1} μM^{-1})	Frequency, f (Hz)	Concentration, $\overline{C}$		Amplitude, A		$A/\overline{C}$ (%)
		μM	mol/cell[b]	μM	mol/cell[b]	
0.209	2	3.17×10^{-5}	50	2.42×10^{-6}	3.79	7.64
0.209	10	1.59×10^{-4}	248	4.02×10^{-7}	0.62	0.25
1.254	2	1.90×10^{-4}	298	1.36×10^{-5}	21.35	7.18
1.254	10	9.48×10^{-4}	1484	2.39×10^{-6}	3.74	0.25

[a]*Input variables*: $L_H = 3.4 \times 10^{-3}$ nM (i.e. $\phi_H = 0.1$ μM/s), $t_H = 20$ ms, $f = 2$ or 10 Hz. *Parameters*: Same as in Table 2 except k_3, either standard (0.209) or increased 6-fold (1.254).

[b]Molecules per cell.

level $C = \overline{C}_c$. The oscillating component calculated in this way is shown in Figure 5. It can be seen that the oscillating component is not identical during the transient and the steady states. However both fluctuate with the same period and with a similar amplitude. So, contrary to the impression given by Figure 3, for example, the oscillations of the ligand concentration are immediately encoded in the oscillations of the signaling complex, although in a distorted way.

Modified parameters for a higher temporal resolution

In order to follow pulses up to 10 Hz, as the cell types responding to the minor pheromone components, the model parameters of Table 2 must be modified. It seems reasonable to modify the parameters so that the amplitude of 3.8 molecules of signaling complex per cell, found at 2 Hz with the previous parameters, is now reached at 10 Hz. This implies that the amplitude of the new system at 2 Hz should be considerably increased. To have larger amplitude, at least one of two conditions must be fulfilled: (i) the system must react faster, i.e. transient state must be shortened; or (ii) the steady-state level must be increased. In the activation pathway (first line of Table 1) these conditions are achieved by changing the forward k_j and backward k_{-j} rate constants (with $j = 2, 3, 4$) for which the ratio $K_j = k_{-j}/k_j$ is large. If K_j is small, the change is not efficient. In the present case, with $K_2 = 0.0638$, $K_3 = 37.46$ and $K_4 = 5.667$, the best results are obtained by increasing k_3, which controls the binding of the loaded PBP to the receptor. In the deactivation pathway (second line of Table 1) the reaction that controls the binding of the loaded PBP to the enzyme N is the most important. Increase of amplitude is achieved by decreasing K_5. Since in differential equations (Appendix A) k_5 always appears in the product k_5N, where N is the constant concentration of enzyme N, it is equivalent to increase k_5 or N. However, any increase of k_5N lengthens the transient state. This slowing down can be compensated by increasing k_6 but then the amplitude is decreased.

Due to these complex effects, the simplest candidate for improving the temporal resolution of the extracellular reaction network is k_3. A 6-fold increase of k_3 with no change of the other parameters results in an amplitude of 3.7 molecules at 10 Hz, with pulses of 3.4×10^{-3} nM (flux 0.1 μM/s) in height (see Discussion) and 20 ms duration as used in experiments (Rumbo and Kaissling, 1989; Kodadová, 1996) (see Table 4). This is approximately the same amplitude as that obtained at 2 Hz with the original value of k_3 without much slowing down the system (the natural period remains approximately the same, see Figure 7). Of course, the average level $\overline{C}$ of the signaling complex does not remain the same; it grows from 50 molecules/cell for $k_3 = 0.209$ (Figure 9A, thick line) to ~1500 molecules/cell for $k_3 = 1.254$ s^{-1} μM^{-1} (Figure 9A, thin line). Interestingly, Figure 9B (dashed line) shows that the resulting fast decline of the relative amplitude $A/\overline{C}$ is not influenced by k_3. Therefore improving relative amplitude can only be attained through the modification of constants other than k_3.

Discussion

Basic properties

Studying how the pheromone sensory system responds to a periodic train of identical pulses offers an idealized equivalent of how a moth 'sees' a pheromone plume when it flies through it. We investigated this problem at the level of the sensory membrane of receptor neurons. All events affecting pheromone molecules up to receptor activation, i.e. translocation from external air to sensillum lymph, transport via PBP, enzymatic deactivation and receptor interactions, were taken into account. However, to simplify the interpretation of the results the transduction of activated receptors into receptor potential was not considered.

We show, using computer simulation of a reaction network model proposed by Kaissling (Kaissling, 2001), that, after a transient state, the concentration of activated receptor proteins (signaling complex) at the surface of receptor neurons oscillates in time around a constant value, with a constant amplitude and with the same period as the stimulus. This is an important feature of the model that

the response can be considered at each instant as the sum of two components, one monotonic (average on time) and the other oscillating, whose properties are very different.

The characteristics of the monotonic component, i.e. the time-averaged concentration of signaling complex and the duration of the transient state, are the simplest to describe because they depend only on the time-averaged amount $\overline{L}$ of ligand delivered to the system, as given by equation (3). Therefore the time-averaged response to a train of pulses is identical to the response to a constant (step) stimulation at concentration L_c of pheromone molecules in the air surrounding the antenna equal to $\overline{L}$. It implies that many different pulse trains differing in their intensity (L_H) and temporal structure (t_H and t_L) yield the same monotonic component of the response, provided they have the same $\overline{L}$. For this reason the quantity $\overline{L}$ of equation (3) appears as a major feature of the pulse trains.

On the contrary, the properties of the oscillating component depend on the detailed characteristics of the pulses, i.e. their height L_H, duration t_H and separation t_L. Although the period of the response is the same as that of the stimulus, $T = t_H + t_L$, its amplitude A is a more complex quantity that depends simultaneously on all three pulse characteristics. However, analysis of the model (see Figure 8) showed that amplitude is influenced much more by period T than by t_H and t_L taken individualy, so that what is important is again the stimulation frequency $f = 1/T$. For example, an increase of t_H compensated by a decrease in t_L which leaves frequency unchanged, is much less influential than the same increase of t_H with unchanged t_L, which increases frequency. This conclusion is valid only for concentrations of the signaling complex far from zero and saturation (see natural period below).

Comparison with other models

Kaissling (Kaissling, 1998a) distinguished two types of chemosensory sensilla, 'concentration detectors' (CDs) and 'flux detectors' (FDs). CDs (Kaissling, 1998a; Lansky *et al.*, 2001; Křivan *et al.*, 2002) are characterized by unrestricted back and forth access of external ligand molecules to the receptor layer, which is not the case of the various FDs in which there is only a forward flux into the perireceptor space compensated by a deactivation of the ligand. The CD model is a realistic description of CO_2-sensitive sensilla, for example, but not of pheromone-sensitive sensilla, which are better described by a FD model. The present 13-reaction system is an example of relatively complex FD. However, it behaves qualitatively like much simpler FDs in which the perireceptor space and reactions taking place in it are considered in a simplified form, and even like CDs for certain properties. For this reason it is interesting to compare the system studied here to these much simpler variants, which differ by the receptor–ligand interactions (CDs and FDs) and the ligand deactivation (FDs only).

For each type of detector, one-step and two-step receptor–ligand interactions were studied. In one-step interaction only the binding of pheromone to receptor, with reaction rates k_3 and k_{-3}, is considered (Kaissling, 1988a,b; Lánský *et al.*, 2001; Křivan *et al.*, 2002), whereas in two-step interaction, binding is followed by activation with reaction rates k_3, k_{-3}, k_{-4} and k_{-4} (Rospars *et al.*, 2000; Kaissling, 2001). As shown below, both one-step and two-step systems are qualitatively, but not quantitatively, equivalent.

Ligand deactivation in FDs was considered as taking place only after the ligand is released from the receptor, the receptor acting as an enzyme, or before the interaction with the receptors, via enzymes present in the sensillum lymph. The first mechanism (receptor-enzyme) was studied by Kaissling (Kaissling, 1998a,b) and Rospars *et al.* (Rospars *et al.*, 2000) and the second one (separate enzymes) by (Kaissling, 1998a, 2001) and in the present paper. A variant of these models, which uses both receptor-enzyme and a flux-limiting process equivalent to separate-enzyme deactivation, is the 'generalized flux detector' (GFD) (Rospars *et al.*, 2000).

Consider first the static properties of these systems, i.e. the dependence of the steady-state concentration $\overline{C}$ on $\overline{L}$. As shown in Appendix B, contrary to Kaissling's conclusion, in both the one-step FD with separate enzyme (Kaissling, 1998a) and the present 13-reaction network (Kaissling, 2001), this dependence is hyperbolic. So, these systems behave qualitatively like CDs, in which the static curve $\overline{C}_c$ vs. L_c is also a hyperbola (Kaissling, 1998a; Rospars *et al.*, 2000). From a quantitative point of view, the closest of the simple models to the present model is the two-step GFD. This is manifest for the position of the static curve along the concentration axis as quantified by the ligand concentration in air at half-maximum response, i.e. the apparent equilibrium dissociation constant K_D. For the one-step CD, it is $K_D = k_{-3}/k_3 = 37.8\ \mu M$, and for the two-step CD, $K_D = k_{-3}k_{-4}/k_3(k_{-4} + k_4) = 32.3\ \mu M$, from equation (13) in Rospars *et al.* (Rospars *et al.*, 2000), whereas it is $K_D \approx 1$ nM for both GFDs and for the present system (equation B5 and Figure 4, with $k_i = 2.9 \times 10^4\ s^{-1}$). So, at steady state, the curve $\overline{C}_c$ vs. $\log L_c$ of all flux detectors is shifted to the left by $\log k_i$, i.e. 4.5 log units, with respect to that of concentration detectors.

The dynamic responses $C(t)$ are qualitatively equivalent in the concentration and flux detectors as can be easily judged by comparing Figure 9 in Rospars *et al.* (Rospars *et al.*, 2000) for the two-step CD, Figure 2 in Křivan *et al.* (Křivan *et al.*, 2002) for the one-step CD and Figure 2 in the present article. But again the quantitative differences are conspicuous, because the 13-reaction system appears slower than those we studied previously. This is best illustrated by the 'natural' period of the system, i.e. the minimum period $t_H + t_L$ such that 'on' and 'off' durations allow for maximum amplitude of the response (see Figure 7). This period is ~12 s, compared with ~1.15 s for both the one-step and two-step CDs, so that the respective 'natural' frequencies are 0.08 and 0.9 Hz. Thus, using the same parameter values, the

present complete FD system is ~10 times slower than the corresponding CDs.

Transient phase

However, the slowness of the 13-reaction system to reach steady state and to return to resting level is not necessarily an important feature as far as pheromone detection is concerned.

First, the rise of the transient monotonic state (dashed line in Figure 3) can be detected without waiting for the steady state. This is probably important in natural conditions where the pulses are irregular in height, duration and separation.

Second, with a a pulse train, the individual pheromonal pulses are also detectable right from the beginning of the transient response, much before the steady-state oscillations are reached. In practice, as shown in Figure 6, the period T and amplitude A can be approximately determined from the first oscillation and, again, there is no need to wait for the steady state. Then the following analysis of amplitude during the steady state holds also true for the amplitude during the transient period.

Amplitude

The dynamic properties of a periodic stimulation are reflected in the amplitude of the signaling-complex oscillations. This is the number of molecules of $LB_{red}R^*$ that are added at each pulse to the time-averaged number of molecules of activated receptor complex.

In the biologically relevant range of pheromone concentrations, amplitude A (see Figure 8C) and relative amplitude $A/\overline{C}$, where $\overline{C}$ is the time-averaged concentration of signaling complex at steady state over one period, have similar properties with respect to stimulation frequency: both decrease quasi-exponentially when frequency is increased. However, they differ radically with respect to pulse height L_H because A increases with L_H (Figure 8A), whereas $A/\overline{C}$ is independent of it (Figure 8B). This implies that amplitude reflects both pulse height and pulse frequency, whereas relative amplitude reflects only frequency.

The neuron type studied, which is sensitive to the main pheromone component, can follow periodic 20 ms pulses up to 2 Hz (Rumbo and Kaissling, 1989; Kodadova, 1996). The stimulating apparatus used in these experiments, loaded with 5×10^{-3} µg of pheromone, was different from the standard one which produced the 2 s step stimulations used for determining the parameters of Table 2. Although the pulse height L_H and corresponding flux delivered by the pulse stimulator were not determined, they are known to be about two orders of magnitude higher for the same load than those of the standard apparatus (Kaissling, personal communication). With this 100-fold factor, the 5×10^{-3} µg load would yield a concentration in air $L_H = 3.4 \times 10^{-3}$ nM and a corresponding flux of 0.1 µM/s. This means, if the present model is essentially correct, that this cell type can detect oscillations of the concentration of signaling complex $LB_{red}R^*$ with amplitude as low as 2.4×10^{-6} µM for a steady-state level of 3.2×10^{-5} (Table 4; Figure 2D). These molarities correspond, for a perireceptor-space volume of 2.6×10^{-12} l (Keil, 1984), to 3.8 receptor molecules oscillating on top of an average level of 50 molecules (Table 4, Figure 9B). These results suggest that the present model, whose parameters were determined from responses to step stimulations of 2 s duration, can also account for periodic pulse stimulations. It constitutes an encouraging independent test of the essential validity of these parameters.

Extensions of the model

The other cell types, sensitive to the minor pheromone components, can resolve pulses up to 10 Hz (Rumbo and Kaissling, 1989). Assuming the same network of extracellular reactions is present in these cells as in the cell type sensitive to the main component, the difference in temporal resolution of pulses can be ascribed to changes in rate constants or initial concentrations of reactants whose effect would be to increase the amplitude of the periodic oscillations of the activated receptor (signaling complex), expressed in both absolute, i.e. number of molecules taking part to the oscillations, and relative terms, i.e. with respect to the total time-averaged number of activated receptors.

Investigation of the sensitivity of the absolute amplitude to parameter values showed that a key factor is the balance between the two pathways that the ligand–PBP complex (LB_{red}) can follow, i.e. either the activation or the deactivation pathway (see Table 1). Although this balance can be modified in several ways, the rate constant k_3, which controls the binding of LB_{red} to the receptor, was found to be a major factor. A 6-fold increase of k_3 from 0.209 to 1.254 s^{-1} μM^{-1} (Table 4), with no change of the other parameters, increases 6-fold the amplitude of the signaling complex at 2 Hz and yields the same amplitude at 10 Hz as the original system at 2 Hz without slowing down of the system (the duration of transient state and the natural period remain the same).

However, modifying k_3 has no influence on relative amplitude, so that the amplitude remains the same small fraction (0.25%) of the average number of activated receptors whatever k_3. It seems unlikely that such a small relative variation can be detected by the cell. The determination of parameters improving both amplitude and relative amplitude which would permit the system to resolve 10 Hz pulses remains an open problem.

The observed decrease of the amplitude of the concentration of the signaling complex when the stimulation frequency increases can be discussed in a wider context. Indeed, Samoilov *et al.* (Samoilov *et al.*, 2002) proved that this is a general property of any linear chemical network driven by a single external oscillatory input signal. All such networks act as low-pass frequency filters. Moreover, their theoretical results show that if a reaction network is

selectively sensitive to some stimulation frequencies (band-pass filtering), then either it has another source of oscillations or it is nonlinear. Since our system is linear only at low ligand concentration, this rises the question of knowing whether the present model could behave as a band-pass filter at high concentration, i.e. a model in which the signaling complex reaches its highest amplitude at some preselected stimulation frequency (e.g. 2 Hz). An alternative approach, used by Lánský *et al.* (Lánský *et al.*, 2001) for a simplified version of the present network, is to consider not only the amplitude of the signaling complex but the product of the amplitude and another variable (speed of change of the amplitude). This product presents a maximum and thus an optimum frequency. This effect, which evokes a band-pass filter, is certainly present also in the network studied here.

Experimental vs. natural conditions

The results reported here are useful for interpreting laboratory experiments in which identical pulses are periodically applied. For example, Figures 2 in Rumbo and Kaissling (Rumbo and Kaissling, 1989) and Kodadová (Kodadová, 1996), showing receptor potential and spike recording of the aldehyde cell under such conditions, are qualitatively comparable to our Figure 3, assuming the receptor potential reflects the level of signaling complex and a spike is fired when this level crosses a certain threshold. However, caution must be exerted in applying them to natural conditions in which the pulses are known to be quite irregular (Murlis *et al.*, 1992). We intend to develop the present approach to study the response of the perireceptor and receptor system to pulses with stochastic characteristics.

Appendix A: differential equations

To avoid notational complexity, all multiple-letter symbols for the various chemical species are replaced by single-letter symbols, i.e. $P = [LB_{red}]$, $O = [LB_{red}R]$, $C = [LB_{red}R^*]$, $\beta = [LB_{ox}]$, $\gamma = [LE]$, $\nu = [LB_{red}N]$, $\eta = [LB_{red}E]$, $\kappa = [LB_{ox}E]$. The other symbols (L, B_{red}, B_{ox}, R, N, E) are kept unchanged. The 10 time-variable concentrations are $L(t)$, $\gamma(t)$, $P(t)$, $R(t)$, $O(t)$, $C(t)$, $\nu(t)$, $\beta(t)$, $\kappa(t)$, $\eta(t)$. All other concentrations R_0, B_{red}, B_{ox}, E, N are constant. With this notation and omitting variable t the system of differential equations describing the model given in Table 1 is

$$\frac{dL}{dt} = k_i L_{air} - k_2 B_{red} L + k_{-2} P - k_7 L B_{ox} + k_{-7}\beta - k_8 L E + k_{-8}\gamma \quad \text{(A1)}$$

$$\frac{d\gamma}{dt} = k_8 L E - k_{-8}\gamma - k_9\gamma \quad \text{(A2)}$$

$$\frac{dP}{dt} = k_2 B_{red} L - k_{-2} P - k_3 P R + k_{-3} O - k_5 P N + k_{-5}\nu - k_{12} P E + k_{-12}\eta \quad \text{(A3)}$$

$$\frac{dO}{dt} = k_3 P R - k_{-3} O - k_4 O + k_{-4} C \quad \text{(A4)}$$

$$\frac{dC}{dt} = k_4 O - k_{-4} C \quad \text{(A5)}$$

$$\frac{d\nu}{dt} = k_5 P N - k_{-5}\nu - k_6\nu \quad \text{(A6)}$$

$$\frac{d\beta}{dt} = k_6\nu + k_7 L B_{ox} - k_{-7}\beta - k_{10}\beta E + k_{-10}\kappa \quad \text{(A7)}$$

$$\frac{d\kappa}{dt} = k_{10}\beta E - k_{-10}\kappa - k_{11}\kappa \quad \text{(A8)}$$

$$\frac{d\eta}{dt} = k_{12} P E - k_{-12}\eta - k_{13}\eta \quad \text{(A9)}$$

$$R = R_0 - O - C \quad \text{(A10)}$$

All time-variable concentrations are equal to zero at time zero, except $R(t)$ for which $R(0) = R_0$.

Species E, N and B are external species, i.e. with constant concentrations despite entering in different reactions, in contrast to R, whose free amount is decreased by bound and activated states. The reaction network is incomplete for L, which accumulates, and for B since B_{red} is not regenerated from the end product MB_{ox} which consequently also accumulates.

Appendix B: receptor concentrations at equilibrium

Differential equations (A1)–(A9) at equilibrium, i.e. for $dL/dt = 0$, $d\gamma/dt = 0$ etc., result in a system of nine algebraic equations with nine unknowns which can be solved exactly. The calculations are long but straightforward. We give here the solutions (B1)–(B3) obtained for the pheromone receptor.

At any time the receptor proteins are in three states, as given by equation (A10): free R, occupied $LB_{red}R$ (denoted O) and activated $LB_{red}R^*$ (denoted C). For a step stimulation L_c, the conservation equation at equilibrium can be written $R_0 = \overline{R}_c + \overline{O}_c + \overline{C}_c$. For a periodic pulsed stimulation, the same equation holds at steady state, $R_0 = \overline{R} + \overline{O} + \overline{C}$, where $\overline{R}$, $\overline{O}$ and $\overline{C}$ are time-averaged concentrations over one period. It can be shown numerically (see Results) that $R = \overline{R}_c$, $O = \overline{O}_c$ and $C = \overline{C}_c$, for $\overline{L} = L_c$, where $\overline{L}$ is the time-averaged concentration of ligand in the air surrounding the antenna, see equation (3). Therefore the following results established for a constant stimulation are also true for the time-averaged response to the equivalent periodic pulsed stimulation. The concentrations of the three receptor states are given by

$$\overline{R}_c = R_0 - \left(\frac{k_4}{k_{-4}} + 1\right)\overline{C}_c \quad \text{(B1)}$$

$$\overline{O}_c = \frac{k_4}{k_{-4}}\overline{C}_c \tag{B2}$$

$$\overline{C}_c = \frac{k_4 R_0 k_i L_c}{(k_4 + k_{-4})k_i L_c + \alpha/\beta} \tag{B3}$$

where

$$\alpha = k_{-3}k_{-4}E(k_8k_9a_4 + k_7k_{10}k_{11}a_2B_{ox})[k_{12}k_{13}a_1E + a_3(k_{-2}a_1 + k_5k6N)] + k_{-3}k_{-4}Ek_2B_{red}a_2(k_{12}k_{13}a_1a_4 + k_{10}k_{11}a_3k_5k6N)$$

$$\beta = k_2k_3a_1a_2a_3a_4B_{red}$$

in which $a_1 = k_{-5} + k_6$, $a_2 = k_{-8} + k_9$, $a_3 = k_{-12} + k_{13}$, $a_4 = k_{10}k_{11}E + (k_{-10} + k_{11})k_{-7}$. For the simplified 10-reaction model characterized by $k_7 = 0$ and $k_{12} = 0$, the expressions for α and β simplify as follows:

$$\alpha = k_{-3}k_{-4}[(k_8k_9E + k_2B_{red}a_2)(k_{12}a_1E + k_5k_6N) + k_{-2}a_1k_8k_9E]$$

$$\beta = a_1a_2k_2k_3B_{red}$$

in which $a_1 = k_{-5} + k_6$, $a_2 = k_{-8} + k_9$.

The concentration of the signaling complex at saturation and the ligand concentration at half-saturation are given by

$$C_{max} = \frac{k_4}{k_4 + k_{-4}}R_0 \tag{B4}$$

$$K_D = \frac{\alpha/\beta}{k_i(k_4 + k_{-4})} \tag{B5}$$

Note that $k_4 + k_{-4}$ (rate constants of receptor activation and deactivation) controls in opposite directions the amount of activated receptor produced and the position of the curve along the L_c-axis (sensitivity). With this notation, equation (B3) reads

$$\overline{C}_c = \frac{C_{max}}{1 + K_D/L_c} \tag{B6}$$

Equations (B3) and (B6) are hyperbolas with respect to L_c (or equivalently ϕ_c). Consequently the curve $\overline{C}_c$ vs. logL_c (or log ϕ_c) is a logistic whose dynamic range is $\Delta L_c \simeq -2 \log \varepsilon$ decades (Rospars *et al.*, 1996), where ε is a fraction of C_{max}. For example, the horizontal distance between 1% (close to threshold) and 99% of C_{max} is always $\Delta L_c = 4$ log units (see Figure 4), so that the ratio of concentrations L_{99}/L_1, (respect. fluxes ϕ_{99}/ϕ_1) at 99% saturation and at 1% threshold is always 10^4, whatever the values of C_{max} and K_D.

With the parameter values given in Table 2, $\alpha/\beta = 3468.4$ $\mu M/s^2$, $C_{max} = 0.24$ μM and $K_D = 1.042$ nM (i.e. flux $\phi_{50} = 30.21$ $\mu M/s$). For a hair volume of 2.6 pl, the total number of molecules per neuron is $R_0 = 2.56 \times 10^6$ and $C_{max} \simeq 3.75 \times 10^5$. The level $\overline{C}_c = 1$ receptor molecule activated (threshold) is reached for a pheromone concentration in air $L_c = 2.8 \times 10^{-6}$ nM corresponding to flux $\phi_c = 8 \times 10^{-5}$ $\mu M/s$, i.e. 125 molecules/s.

For $L_c << K_D$, hyperbola (B6) can be approximated by the linear expression

$$\overline{C}_c \approx \frac{C_{max}}{K_D}L_c \tag{B7}$$

or, using fluxes, $\overline{C}_c \approx (C_{max}/\phi_{50})\phi_c$. The slope of line (B7) is

$$\frac{C_{max}}{K_D} = \frac{k_i k_4 R_0}{\alpha/\beta} \tag{B8}$$

With the parameter values of Table 2, $C_{max}/K_D = 0.23$ with K_D and L_c in nM, and C_{max} and $\overline{C}_c$ in μM, and for the flux equation the slope is $\phi_{50}/C_{max} = 125.9$ with all terms in μM. With these parameters the hyperbola is rather flat (see Figure 4A) so that, in practice, the line $\overline{C}_c = \phi_c/126$ (i.e. $0.23L_c$) is an excellent approximation in the range $0 \le \phi_c \le 1$ $\mu M/s$. The line $\overline{C}_c = \phi_c/150$ (i.e. $0.19L_c$), as used by Kaissling (Kaissling, 2001), is a better approximation for $\phi_c > 1$ $\mu M/s$.

Note. The equation relating ϕ_c to $\overline{C}_c$ was also derived as equation (4) in Kaissling (Kaissling, 2001) for the present 13-reaction system, and as equation (18) in Kaissling (Kaissling, 1998a) for a simplified three-reaction network with one-step activation and a separate enzyme. In both cases the system of differential equations describing the networks are correct but the equations giving $\overline{C}_c$ at equilibrium are not. The exact solutions for $\overline{C}_c$ are hyperbolic functions of the form (B6), i.e. the –1 term appearing in the denominator of both equations (18) and (4) must be removed. Because of this term, it was wrongly concluded that the $\overline{C}_c$ vs. ϕ_c curves were not hyperbolic and that there was a limiting flux ϕ_{sat}. Other consequences will be examined elsewhere (K.-E. Kaissling and J.-P. Rospars, in preparation).

Acknowledgements

The authors thank K.-E. Kaissling for unpublished data, helpful discussions and constructive criticisms on earlier versions of this manuscript. This work was partly supported by joint cooperation project Barrande No. 972SL between France and the Czech Republic, by NATO linkage grant LST CLG 976786, by Grant Agency of the Czech Republic (309/02/0168), by Grant Agency of ASCR (Z5007907) and by MSMT (12300004).

References

Christensen, T.C. and **Hildebrand, J.G.** (1988) *Frequency coding by central olfactory neurons in the sphinx moth* Manduca sexta. Chem. Senses, 13, 123–130.

Kaissling, K.-E. (1987) R.H. Wright Lectures on Insect Olfaction. Simon Fraser University, Burnaby.

Kaissling, K.-E. (1998a) *Flux detectors vs. concentration detectors: two types of chemoreceptors*. Chem. Senses, 23, 99–111.

Kaissling, K.-E. (1998b) *Pheromone deactivation catalyzed by receptor molecules: a quantitative kinetic model*. Chem. Senses, 23, 385–395.

Kaissling, K.-E. (2001) *Olfactory perireceptor and receptor events in moth: a kinetic model.* Chem. Senses, 26, 125–150.

Keil, T.A. (1984) *Reconstruction and morphometry of silkmoth olfactory hairs: a comparative study of sensilla trichodea on the antennae of male* Antheraea polyphemus *and* Antheraea pernyi *(Insecta, Lepidoptera).* Zoomorphology, 104, 147–156.

Kennedy, J.S., Ludlow, A.R. and **Sanders, C.J.** (1980) *Guidance system used in moth sex attraction*. Nature, 288, 474–477.

Kennedy, J.S., Ludlow, A.R. and **Sanders, C.J.** (1981) *Guidance of flying male moths by wind-borne sex pheromone.* Physiol. Entomol., 6, 395–412.

Kodadová, B. (1996) *Resolution of pheromone pulses in receptor cells of* Antheraea polyphemus *at different temperatures.* J. Comp. Physiol. A, 179, 301–330.

Kramer, E. (1986) *Turbulent diffusion and pheromone-triggered anemotaxis*. In Payne, T.L., Birch, M.C. and Kennedy, C.E.J. (eds), Mechanisms in Insect Olfaction. Clarendon Press, Oxford, pp. 59–67.

Kramer, E. (1992) *Attractivity of pheromone surpassed by time-patterned application of two nonpheromone compounds.* J. Insect Behav., 5, 83–97.

Krivan, V., Lánský, P. and **Rospars, J.-P.** (2002) *Coding of periodic pulse stimulation in chemoreceptors.* BioSystems, 67, 121–128.

Lánský, P., Krivan, V. and **Rospars, J.-P.** (2001) *Ligand interaction with receptors under periodic stimulation: a modeling study with application to concentration chemoreceptors.* Eur. Biophys. J., 30, 110–120.

Marion-Poll, F. and **Tobin, T.R.** (1992) *Temporal coding of pheromone pulses and trains in* Manduca sexta. J. Comp. Physiol. A, 171, 505–512.

Meng, L.Z., Wu, C.H., Wicklein, M., Kaissling, K.E. and **Bestmann, H.J.** (1989) *Number and sensitivity of three types of pheromone receptor cells in* Antheraea pernyi *and* A. polyphemus. J. Comp. Physiol. A, 165, 139–146.

Murlis, J.S., Elkinton, J.S. and **Cardé, R.T.** (1992) *Odor plumes and how insects use them*. Annu. Rev. Entomol., 37, 505–532.

Pelosi, P. and **Maida, R.** (1995) *Odorant-binding proteins in insects*. Comp. Biochem. Physiol., 111, 503–514.

Rospars, J.-P., Lánský, P., Tuckwell, H.C. and **Vermeulen, A.** (1996) *Coding of odor intensity in a steady-state deterministic model of an olfactory receptor neuron*. J. Comput. Neurosci., 3, 51–72

Rospars, J.-P., Krivan, V. and **Lánský, P**. (2000) *Perireceptor and receptor events in olfaction. Comparison of concentration and flux detectors: a modeling study*. Chem Senses, 25, 293–311.

Rumbo, E.R. and **Kaissling, K.-E.** (1989) *Temporal resolution of odour pulses by three types of pheromone receptor cells in* Antheraea polyphemus. J. Comp. Physiol. A, 165, 281–291.

Samoilov, M., Arkin, A. and **Ross, J.** (2002) *Signal processing by simple chemical systems.* J. Phys. Chem. A, 106, 10205–10221.

Steinbrecht, R.A. (1997) *Pore structures in insect olfactory sensilla: a review of data and concepts.* Int. J. Insect Morphol. Embryol., 26, 229–245.

Stengl, M., Ziegelberger, G., Boekhof, I. and **Krieger, J.** (1999) *Perireceptor events and transduction mechanisms in insect olfaction*. In Hansson, B.S. (ed.), Insect Olfaction. Springer Verlag, Berlin, pp. 49–66.

Vickers, N.J. and **Baker, T.C.** (1992) *Male* Heliothis virescens *maintain upwind flight in response to experimentally pulsed filaments of their sex pheromone (Lepidoptera, Noctuidae)*. J. Insect Behav., 5, 699–687.

Willis, M.A. and **Baker T.C.** (1984) *Effects of intermittent and continuous pheromone stimulation on the flight behavior of the oriental fruit moth,* Grapholita molesta. Physiol. Entomol., 9, 341–358.

Zeigelberger, G. (1995) *Redox-shift of pheromone-binding protein in the silkmoth* Antheraea polyphemus. Eur. J. Biochem., 232, 706–711.

Accepted May 31, 2003